

University of Wollongong

Research Online

Faculty of Science, Medicine and Health -
Papers: part A

Faculty of Science, Medicine and Health

1-1-2013

Does addition of NO₂ to carbon-centered radicals yield RONO or RNO₂? An investigation using distonic radical ions

Benjamin B. Kirk

University of Wollongong, bkirk@uow.edu.au

Adam J. Trevitt

University of Wollongong, adamt@uow.edu.au

Stephen J. Blanksby

University of Wollongong, blanksby@uow.edu.au

Follow this and additional works at: <https://ro.uow.edu.au/smhpapers>



Part of the [Medicine and Health Sciences Commons](#), and the [Social and Behavioral Sciences Commons](#)

Recommended Citation

Kirk, Benjamin B.; Trevitt, Adam J.; and Blanksby, Stephen J., "Does addition of NO₂ to carbon-centered radicals yield RONO or RNO₂? An investigation using distonic radical ions" (2013). *Faculty of Science, Medicine and Health - Papers: part A*. 615.

<https://ro.uow.edu.au/smhpapers/615>

Research Online is the open access institutional repository for the University of Wollongong. For further information contact the UOW Library: research-pubs@uow.edu.au

Does addition of NO₂ to carbon-centered radicals yield RONO or RNO₂? An investigation using distonic radical ions

Abstract

Nitrogen dioxide is used as a "radical scavenger" to probe the position of carbon-centered radicals within complex radical ions in the gas phase. As with analogous neutral radical reactions, this addition results in formation of an $[M + \text{NO}_2]^+$ adduct, but the structural identity of this species remains ambiguous. Specifically, the question remains: do such adducts have a nitro-(RNO₂) or nitrosoxy-(RONO) moiety, or are both isomers present in the adduct population? In order to elucidate the products of such reactions, we have prepared and isolated three distonic phenyl radical cations and observed their reactions with nitrogen dioxide in the gas phase by ion-trap mass spectrometry. In each case, stabilized $[M + \text{NO}_2]^+$ adduct ions are observed and isolated. The structure of these adducts is probed by collision-induced dissociation and ultraviolet photodissociation action spectroscopy and a comparison made to the analogous spectra of authentic nitro- and nitrosoxy-benzenes. We demonstrate unequivocally that for the phenyl radical cations studied here, all stabilized $[M + \text{NO}_2]^+$ adducts are exclusively nitrobenzenes. Electronic structure calculations support these mass spectrometric observations and suggest that, under low-pressure conditions, the nitrosoxy-isomer is unlikely to be isolated from the reaction of an alkyl or aryl radical with NO₂. The combined experimental and theoretical results lead to the prediction that stabilization of the nitrosoxy-isomer will only be possible for systems wherein the energy required for dissociation of the RO-NO bond (or other low energy fragmentation channels) rises close to, or above, the energy of the separated reactants.

Keywords

centered, radicals, yield, rono, rno₂, investigation, distonic, radical, ions, does, no₂, addition, carbon, GeoQuest

Disciplines

Medicine and Health Sciences | Social and Behavioral Sciences

Publication Details

Kirk, B. B., Trevitt, A. J. & Blanksby, S. J. (2013). Does addition of NO₂ to carbon-centered radicals yield RONO or RNO₂? An investigation using distonic radical ions. *Journal of the American Society for Mass Spectrometry*, 24 (4), 481-492.

**Does addition of NO₂ to carbon-centered radicals yield RONO or
RNO₂? An investigation using distonic radical ions**

Benjamin B. Kirk,[†] Adam J. Trevitt,[†] Stephen J. Blanksby^{†*}

* Corresponding Author

ARC Centre of Excellence for Free Radical Chemistry and Biotechnology, University of Wollongong,
NSW 2522, Australia.

[†] School of Chemistry, University of Wollongong, NSW 2522, Australia

Abstract

Nitrogen dioxide is used as a “radical scavenger” to probe the position of carbon-centered radicals within complex radical ions in the gas phase. As with analogous neutral radical reactions, this addition results in formation of an $[M+NO_2]^+$ adduct, but the structural identity of this species remains ambiguous. Specifically, the question remains: do such adducts have a nitro- (RNO_2) or nitrosoxy- ($RONO$) moiety, or are both isomers present in the adduct population? In order to elucidate the products of such reactions, we have prepared and isolated three distonic phenyl radical cations and observed their reactions with nitrogen dioxide in the gas phase by ion-trap mass spectrometry. In each case, stabilized $[M + NO_2]^+$ adduct ions are observed and isolated. The structure of these adducts is probed by collision-induced dissociation and ultraviolet photodissociation action spectroscopy and a comparison made to the analogous spectra of authentic nitro- and nitrosoxy-benzenes. We demonstrate unequivocally that, for the phenyl radical cations studied here, all stabilized $[M + NO_2]^+$ adducts are exclusively nitrobenzenes. Electronic structure calculations support these mass spectrometric observations and suggest that, under low-pressure conditions, the nitrosoxy-isomer is unlikely to be isolated from the reaction of an alkyl or aryl radical with NO_2 . The combined experimental and theoretical results lead to the prediction that stabilization of the nitrosoxy-isomer will only be possible for systems wherein the energy required for dissociation of the RO-NO bond (or other low energy fragmentation channels) rises close to, or above, the energy of the separated reactants.

Introduction

The reaction of alkyl and aryl radicals (R) with nitrogen dioxide (NO₂) has been extensively studied in the context of combustion and atmospheric chemistries [1,2,3]. It is reported to proceed by barrierless radical addition to generate a nitroalkane or nitroarene (RNO₂). The nascent vibrationally excited species may be (1) stabilized by collisions, (2) eject nitrous acid (HONO), or (3) isomerize to the corresponding nitrite (RONO) which may then go on to (4) eject NO to form an alkoxy or aryloxy radical.



It is generally reported that the end products of alkyl radical + NO₂ reactions are a mixture of all four pathways, with all reaction pathways proceeding *via* initial formation of the nitroalkane [2,3,4], while reaction of aryl radicals with NO₂ results in reactions (1), (3) and (4) [5]. Kinetic data have been reported for the reaction of a number of short chain alkyl radicals with NO₂ in flow-tube experiments based primarily on depletion of the parent radical. Experimental determination of the reaction products was difficult, however, as the nitro and nitrite isomers are prone to dissociative photoionization [2,3].

Xu and Lin proposed that NO₂ could add to the phenyl radical *via* oxygen to directly generate nitrosoxybenzene [4]. It is unclear, however, whether this proceeds without barrier, as the unpaired electron in NO₂ formally resides on the nitrogen in the ground $\tilde{X}(^2A_1)$ state. Significant energy (27.8 ± 0.2 kcal/mol [6]) is thus required to access the $\tilde{A}(^2B_2)$ excited state where the electron resides on oxygen such as to facilitate a barrierless radical addition *via* oxygen. Ellison *et*

al. proposed a two-state diabatic model to rationalize the F + NO₂ reaction surface where an avoided crossing between the ground and excited state of NO₂ lowers the association barrier to the nitrite (FONO) from 27.8 ± 0.2 kcal/mol to 22 ± 3 kcal/mol [7]. It is unknown whether a similar model is applicable for reaction of the phenyl radical with NO₂; however, one would not expect this barrier to disappear entirely.

In a recent mass spectrometric study, Barlow and co-workers used NO₂ as a “radical scavenger” [8] to probe the location of a carbon-centered radical (R) generated during collision-induced dissociation (CID) of ionized peptide nitrate esters (*i.e.*, R-CH₂ONO₂ → R + CH₂O + NO₂) [9]. Reaction of the nascent peptidyl radical cation was reported to form an [M + NO₂]⁺ adduct. Subsequent CID of this adduct resulted in loss of HONO, in addition to fragment ions consistent with ejection of NO and concomitant β-scission of the nascent alkoxy radical (*i.e.*, an [M + NO₂ - NO]⁺ fragment ion was not directly observed). While this CID behavior might be considered as evidence for the nitrosoxy (RONO) structure in the adduct ion, activation of nitro (RNO₂) compounds has also been shown to facilitate isomerization to the nitrite with analogous ejection of NO [10,11,12,13,14]. As such, loss of NO (or related fragments) is not an unambiguous diagnostic for the presence of a nitrosoxy moiety. In this radical ion study therefore, as found in previous neutral radical experiments [2,3], the unequivocal assignment of the [M + NO₂]⁺ adduct to either the nitro or nitrite could not be made.

With this in mind, we have investigated the reaction of NO₂ with simple distonic phenyl radical cations to elucidate the products of such reactions. In these experiments, we (i) observe the reaction of distonic phenyl radical cations with NO₂; (ii) probe the structure the resulting [M + NO₂]⁺ adduct by CID and ultraviolet photodissociation (UVPD) action spectroscopy; and (iii) compare these spectra to those obtained from the authentic nitrobenzene and nitrosoxybenzene. We demonstrate unequivocally that reaction of these distonic phenyl radicals with NO₂ generates the charge-tagged nitrobenzene.

Experimental

Materials

4-nitroaniline and HPLC grade methanol were purchased from Ajax Finechem (Sydney, Australia). Nitrogen dioxide (NO₂) was generated from the reaction of nitric oxide (NO) with oxygen (O₂) on a 50 mL scale in a gas-tight syringe, as described previously by Mattson [15]. Nitric oxide (NO) was purchased from Sigma Aldrich (98.5%, St. Louis, MO). Industrial grade oxygen (O₂) was purchased from BOC (> 99.5%, Sydney, Australia). The target distonic radical cations **A**, **B** and **C** were prepared from the precursors: *N,N,N*-trimethyl-2-((2-thioxopyridin-*N*-yloxy)carbonyl)benzeneaminium iodide; 3-iodo-*N,N,N*-trimethylbenzaminium iodide; and 1-(4-iodophenyl)-*N,N,N*-trimethylmethanaminium iodide, synthesized as described previously [16].

Synthesis of N,N,N-trimethyl-4-nitrobenzaminium iodide

4-nitroaniline (200 mg, 1.45 mmol) and potassium carbonate (200 mg, 1.45 mmol) were added to iodomethane (900 µL, 14.5 mmol) and stirred at 40 °C for 24 hours. The iodomethane was removed *in vacuo* and 1 mg of the resulting yellow powder was partitioned between water (1 mL) and CHCl₃ (1 mL). The CHCl₃ layer was discarded and the water layer diluted in MeOH. While the preceding methylation did not produce an isolable product, there was sufficient *N,N,N*-trimethyl-4-nitrobenzaminium iodide generated *in situ* for characterization by tandem mass spectrometry (*vide infra*).

Mass Spectrometry

Methanolic solutions of precursor compounds were prepared at 10-50 µM concentrations and infused at a rate of 3-5 µL/min into the electrospray ionization source of a Thermo Fisher Scientific

LTQ linear quadrupole ion-trap mass spectrometer (San Jose, CA). The linear ion-trap mass spectrometer has previously been modified to perform both photodissociation [17,18] and ion-molecule reactions [19]. Typical source parameters were: spray voltage +3.0-4.5 kV; capillary temperature 200-250 °C; sheath gas flow between 10 and 30 (arbitrary units); and sweep and auxiliary gas flow set at between 0 and 10 (arbitrary units). For collision experiments, ions were mass-selected with a window of 1-4 Th and fragmented using default instrument parameters, *i.e.*, 0.250 activation Q, 30 ms excitation time, unless otherwise noted. Normalized collision energies were optimized for each CID experiment and are noted in relevant spectra. All spectra presented are an average of at least 50 scans.

Photodissociation

The linear ion-trap mass spectrometer has been modified as described elsewhere [17,18,20]. Briefly, a 2.75 in. quartz viewport (MDC Vacuum Products, Hayward, CA) is affixed to the back plate of the spectrometer vacuum housing with a CF flange to allow irradiation of trapped ions with a laser pulse. Two laser systems are utilized; (i) a fixed frequency 266 nm laser for generation of radicals; and (ii) a tunable OPO laser (215 – 320 nm) system used when measuring ultraviolet photodissociation (UVPD) action spectra [21].

The fixed frequency 266 nm laser pulse (fluence = 35 mJ/cm²) is generated by a flashlamp-pumped Nd:YAG laser (Minilite II, Continuum, Santa Clara, CA). Two right-angle prisms direct the laser pulse into the ion trap and are adjusted to optimize overlap with the ion cloud. A TTL pulse generated at the beginning of the MSⁿ activation step triggers the laser flashlamp such that only a single laser pulse is generated per duty cycle.

Tunable UV radiation (213 – 354 nm) is generated by an OPO laser system fitted with a frequency-doubling unit (versaScan and uvScan, Spectra-Physics, Santa Clara, CA, USA). The OPO is pumped by the 3rd harmonic (355 nm) of a Quanta-Ray INDI Nd:YAG laser (Spectra-Physics, Santa Clara, CA,

USA). The OPO-generated UV laser pulse is noticeably divergent in one dimension and this is corrected using a single cylindrical quartz lens. Two quartz prisms are adjusted to ensure good overlap between the UV laser pulse and the ion cloud. The laser is operated continuously at 10 Hz. To ensure that only a single laser-pulse irradiates ions in the trap at the desired MS interval, a mechanical shutter is placed before the LTQ window and is synchronized to open for ~100 ms using a TTL pulse generated during the activation step of an MSⁿ cycle [20]. The normalized collision energy during this activation step is maintained at 0 (arbitrary units) such that product ions measured are generated solely by UVPD. Photoproduct yields are calculated using: *product yield* = ($\Sigma product_{\lambda}/TIC_{\lambda}$), where $\Sigma product$ is the abundance of all photofragments, *TIC* the total ion count at wavelength λ . The laser power spectrum is measured using a thermopile power meter and is typically between 0.2 - 1.1 mJ/pulse. A UVPD action spectrum is obtained by plotting the UVPD product yield against wavelength. It is important to note that the OPO beam intensity spatial profile may vary over this wavelength range and it is difficult to account for the overlap efficiency between the ion ensemble and the laser beam. Therefore, we correct the photoproduct yield for the laser power profile over the wavelength range but not for absolute laser power. Experiments herein were undertaken consecutively to generate comparable data under these conditions. This allows us to confidently compare photoproduct yields between action spectra while minimizing the effects of temporal fluctuations in the laser power or beam profile.

Ion-molecule reactions

Modifications to the linear ion-trap mass spectrometer that allow the introduction of neutral gases into the ion-trap region of the instrument have been described previously [19]. Briefly, reagent gases in a syringe are introduced into a flow of Ultra High Purity (UHP) helium (3-5 psi) *via* a heated septum inlet (25-250 °C). The gas mixture is introduced into the ion trap *via* a variable leak valve, which is adjusted to set an ion trap pressure of ~2.5 mTorr. The temperature of the vacuum

manifold surrounding the ion trap was measured at 307 ± 1 K, which is taken as being the effective temperature for ion-molecule reactions observed therein [19,22] Reaction times of 30-10000 ms were set using the excitation time parameter within the control software using a normalized collision energy of 0 (arbitrary units).

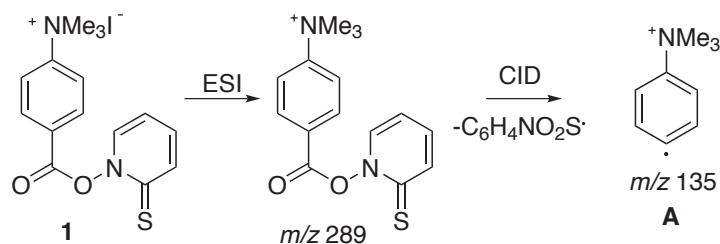
Electronic structure calculations

All calculations were undertaken using the hybrid density functional theory B3LYP method [23,24] and the aug-cc-pVDZ basis set [25] within the GAUSSIAN09 suite of programs [26]. All stationary points on the potential energy surface were characterized as either minima (no imaginary frequencies) or transition states (one imaginary frequency) by calculation of the frequencies using analytical gradient procedures. Minima between transition states were confirmed by calculation of the intrinsic reaction coordinate (IRC) [27,28,29]. Calculated energies (ΔH_0) include unscaled zero-point energy, while Gibbs free energies (ΔG_{298}) include free energy corrections calculated at a temperature of 298.15 K and pressure of 1.0 atm.

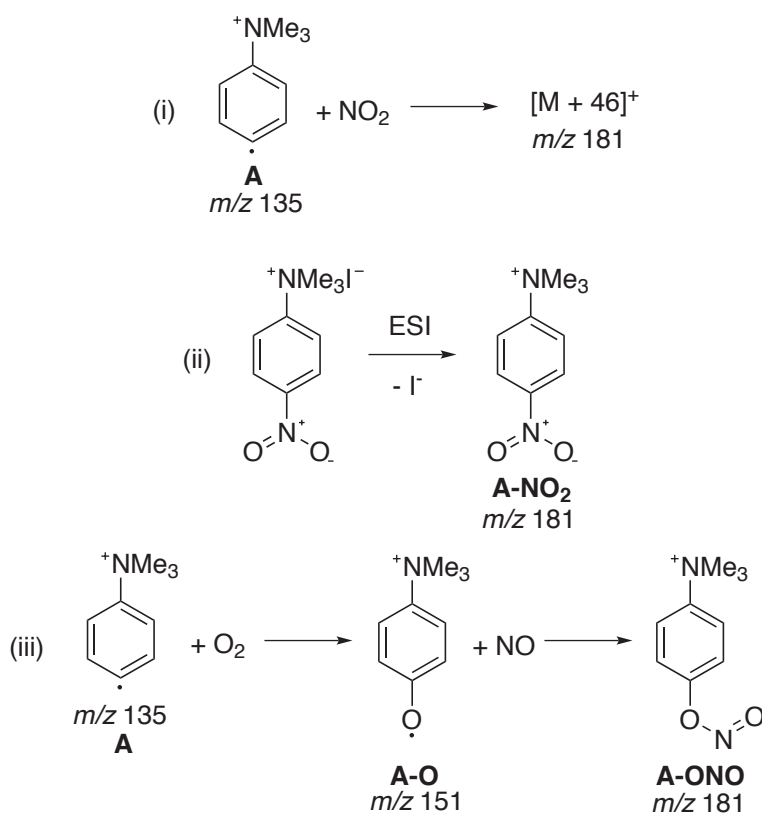
Results

*Preparation of 4-(*N,N,N*-trimethylammonium)phenyl radical cation (**A**)*

N,N,N-trimethyl-2-((2-thioxopyridin-*N*-yloxy)carbonyl)benzeneaminium iodide (**1**) was infused via positive electrospray ionization to generate the *N,N,N*-trimethyl-2-((2-thioxopyridin-*N*-yloxy)carbonyl)benzeneaminium cation at m/z 289. Subjecting this cation to a single laser shot (266 nm, 2.4 mJ/pulse) or collision-induced dissociation (CID) resulted in formation 4-(*N,N,N*-trimethylammonium)phenyl radical cation (**A**) at m/z 135 (Scheme 1). Previous experiments within our laboratory have demonstrated that both PD and CID of **1** generate **A** [16,30]. For all experiments subsequently described we have used CID exclusively to generate **A**.



Scheme 1 - Electrospray ionization (ESI) of *N,N,N*-trimethyl-2-((2-thioxopyridin-*N*-yloxy)carbonyl)benzeneaminium iodide (**1**) and CID of the resulting *N,N,N*-trimethyl-2-((2-thioxopyridin-*N*-yloxy)carbonyl)benzeneaminium cation at *m/z* 289 results in generation of the 4-(*N,N,N*-trimethylammonium)phenyl radical at *m/z* 135 (**A**).



Scheme 2 – Gas-phase synthesis of isomeric *m/z* 181 ions including: (i) the $[\text{M} + 46]^+$ ion arising from reaction of 4-(*N,N,N*-trimethylammonium)phenyl radical cation with NO_2 ; the generation of authentic (ii) *N,N,N*-trimethyl-4-nitrobenzaminium cation; and (iii) *N,N,N*-trimethyl-4-nitrosoxybenzaminium cation (**A-ONO**) by reaction of 4-(*N,N,N*-trimethylammonium)phenoxy radical cation (**A-O**) with NO .

Reaction of charge-tagged phenyl radicals with NO₂

The 4-(*N,N,N*-trimethylammonium)phenyl radical cation (**A**) was allowed to react with NO₂ that was seeded into the helium buffer gas of the mass spectrometer. A typical mass spectrum obtained from this reaction is shown in Figure 1 and reveals an abundant [M + NO₂]⁺ adduct ion at *m/z* 181 (Scheme 2i). Stabilization of either charge-tagged nitro- (**A-NO₂**) or nitrosoxybenzene (**A-ONO**) could account for this signal and, thus, the identity of this ion remains to be established (*vide infra*). Additional ions present in this spectrum include: [M + 1]⁺, [M + 16]⁺, [M + 30]⁺ and [M + 32]⁺ ions at *m/z* 136, 151, 165 and 167, respectively, that arise due to reaction of **A** with background O₂ or unreacted NO (present in the synthetic NO₂). The [M + 16]⁺ and [M + 32]⁺ ions have previously been observed from reaction of **A** with O₂ and correspond to the phenoxy and phenylperoxy radicals, respectively [16,30]. The [M + 30]⁺ ion at *m/z* 165 suggests the presence of unreacted NO and is assigned as an [M + NO]⁺ adduct. Interestingly, the phenoxy radical at *m/z* 151 ion is significantly enhanced compared to previous observations of the **A** + O₂ reaction in the absence of NO_x [16,30]. This enhancement may arise due to a reaction between the peroxy radical at *m/z* 167 and NO or NO₂ by analogy with the well-established neutral reactivity [31]. Alternatively *m/z* 151 could arise directly by NO ejection from energetic [M + NO₂]⁺ adducts (*vide infra*) [1,4]. Exothermic formation of the phenoxy radical by either mechanism could drive subsequent CH₃ loss, therefore, the [M + 1]⁺ ion is assigned as the [M + 16 – CH₃]⁺ ion.

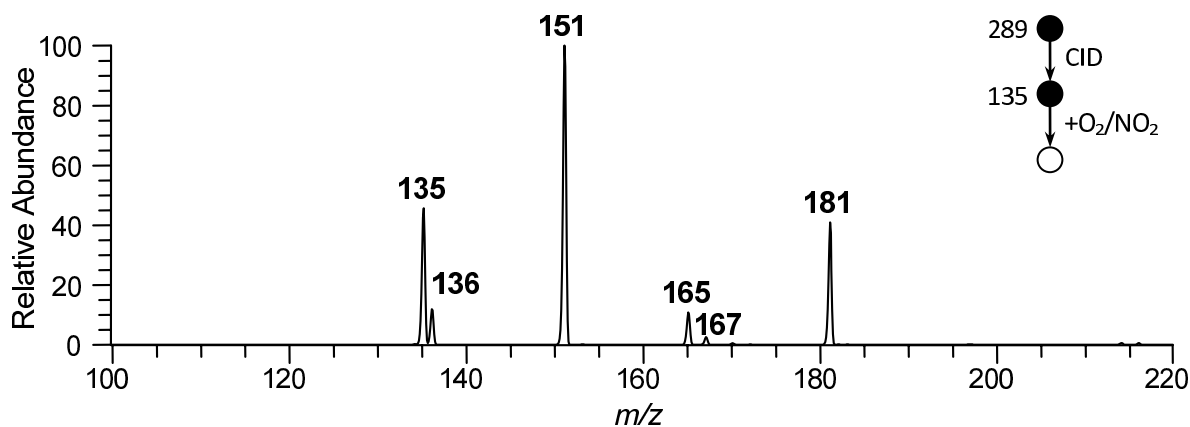


Figure 1 – A mass spectrum obtained following the gas-phase reaction of the 4-(*N,N,N*-trimethylammonium)phenyl radical cation (**A**) with NO_2 . An $[\text{M} + 46]^+$ adduct is observed at m/z 181 consistent with addition of NO_2 to the phenyl radical.

Independent synthesis of nitrobenzene (A-NO₂) and nitrosoxybenzene (A-ONO) analogues in the gas phase.

A solution containing *N,N,N*-trimethyl-4-nitrobenzaminium iodide was infused *via* positive ion electrospray ionization to yield an abundant ion at m/z 181 consistent with the target *N,N,N*-trimethyl-4-nitrobenzaminium cation (**A-NO₂**) (Scheme 2ii).

Previous studies by Yu *et al.* [32], Berho *et al.* [33] and Platz *et al.* [34] have shown that reaction of phenoxy radical with NO generates nitrosoxybenzene. The reaction was employed here to generate the charge-tagged nitrosoxybenzene analogue. In this synthesis, the 4-(*N,N,N*-trimethylammonium)phenyl radical cation (**A**) was allowed to react in the presence of NO (seeded into the helium buffer gas) and O_2 (present in background concentrations), resulting in formation of a number of ions, including the 4-(*N,N,N*-trimethylammonium)phenoxy radical cation (**A-O**) at m/z 151. The charge-tagged phenoxy radical (**A-O**) was then isolated and allowed to react further in the same gas atmosphere. A mass spectrum acquired under these conditions is shown in Figure 2 and

reveals formation of an $[M + 30]^+$ adduct at m/z 181 assigned as the *N,N,N*-trimethyl-4-nitrosoxybenzaminium cation (**A-ONO**) (Scheme 2iii).

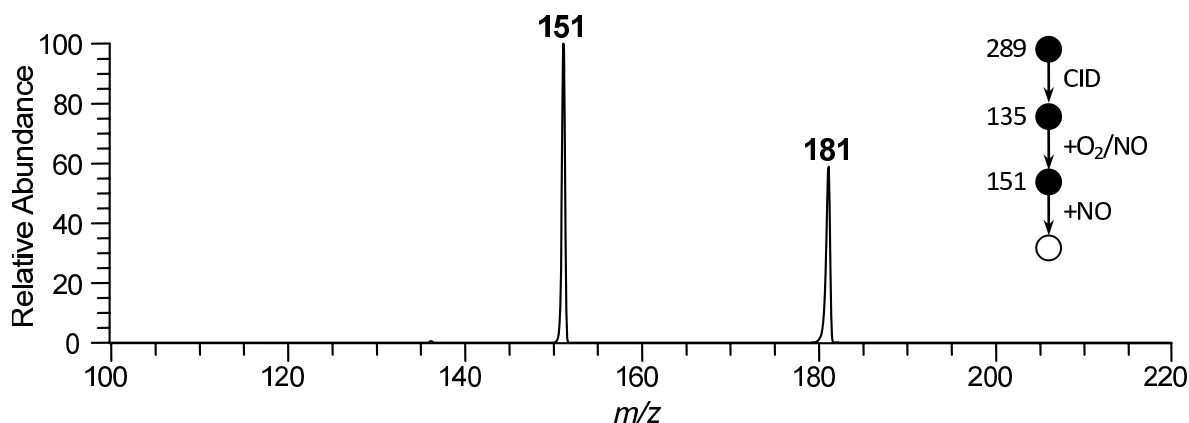


Figure 2 – A mass spectrum obtained following the gas-phase reaction of the 4-(*N,N,N*-trimethylammonium)phenoxy radical cation (**A-O**) with NO. An $[M + 30]^+$ adduct is observed at m/z 181 consistent with addition of NO to **A-O** and is assigned as *N,N,N*-trimethyl-4-nitrosoxybenzaminium cation (**A-ONO**).

Comparison of CID and UVPD spectra

Figures 3(a-c) depict CID spectra of the three m/z 181 ions generated by the pathways outlined in Scheme 2, namely: (i) reaction of the 4-(*N,N,N*-trimethylammonium)phenyl radical cation (**A**) with NO_2 ; (ii) genuine 4-nitro-*N,N,N*-trimethylbenzaminium cation (**A-NO₂**); and (iii) *N,N,N*-trimethyl-4-nitrosoxybenzaminium cation (**A-ONO**). A typical CID spectrum of the $[M + \text{NO}_2]^+$ adduct is depicted in Figure 3(a) and features $[M - 15]^+$, $[M - 16]^+$, $[M - 30]^+$, $[M - 45]^+$ and $[M - 36]^+$ ions assigned as $[M - \text{CH}_3]^+$, $[M - \text{O}]^+$, $[M - \text{NO}]^+$, $[M - \text{NO} - \text{CH}_3]^+$ and $[M - \text{NO}_2]^+$ ions, respectively. In contrast, the CID spectrum of **A-ONO** shown in Figure 3(c) features a single product ion at m/z 151 arising due to loss of NO to form a phenoxy radical. In addition, the normalized collision energy used to generate this spectrum was significantly lower at CE = 15 (arbitrary units) indicating that loss of NO in this

case requires significantly less energy than fragmentation pathways observed after CID of the $[M + \text{NO}_2]^+$ adduct, consistent with a low bond dissociation energy for the RO-NO bond in a nitrosoxybenzene [4]. The CID spectrum of **A-NO₂** depicted in Figure 3(b) is identical to the CID spectrum of the $[M + \text{NO}_2]^+$ adduct obtained at the same collision energy (Figure 3a). When the CID spectrum of the $[M + \text{NO}_2]^+$ adduct is measured at CE = 15 (arbitrary units), for comparison with Figure 3(c) (data not shown), no product ions are generated indicating there is no contribution from **A-ONO** in the m/z 181 ion population. The $[M - 30]^+$ ion generated in Figure 3(a) and (b) must therefore arise due to either (i) a significantly higher energy process, *e.g.*, isomerization of the nitrobenzene to the nitrosoxybenzene with concomitant ejection of NO, or (ii) addition of O₂/NO to the phenyl radical at m/z 135 regenerated upon activation (*c.f.* Figure 1). There was no $[M - 30]^+$ ion in the CID spectrum measured of authentic **A-NO₂** without NO present in the helium buffer gas (Supporting Information, Figure S2), which suggests the ion at m/z 151 arises due to (ii). However, the $[M - 45]^+$ ion at m/z 136 remained at a similar abundance to that observed in Figure 3(b), suggesting this ion arises due to (i), *i.e.*, isomerisation of **A-NO₂** to **A-ONO** followed by loss of NO and subsequent CH₃ ejection, or alternatively, loss of CH₃ followed by subsequent NO ejection.

Representative UVPD mass spectra recorded at 225 nm for all three isomeric m/z 181 ions are presented in Figures 4(a-c). Fragment ions featured in Figures 4(a) and (b) are similar to those present in the corresponding CID spectra (*c.f.* Figures 3a and 3b, respectively). The UVPD mass spectrum shown in Figure 4(c) measured after PD of **A-ONO** reveals an $[M - 30]^+$ ion at m/z 151 assigned as the charge-tagged phenoxy radical arising due to ejection of NO. In addition, an $[M - 45]^+$ ion featured at m/z 136 arises due to subsequent CH₃ loss from the nascent phenoxy radical. This additional fragmentation channel is presumably driven, in addition to electronic effects, by the considerable excess energy imparted on the parent ion during PD (225 nm = 127.2 kcal/mol), in contrast to the “slow-heating” activation of CID [35].

A series of UVPD mass spectra for the $[M + \text{NO}_2]^+$ adduct, **A-NO₂** and **A-ONO** were acquired over a wavelength range between 215 – 320 nm in increments of 1 nm between 215 - 240 nm and 5 nm between 240 – 320 nm. Plotting the power-corrected photoproduct yield as a function of wavelength results in the UVPD action spectra depicted in Figures 5(a-c). The UVPD action spectrum measured for the $[M + \text{NO}_2]^+$ adduct (Figure 5a, green diamonds) reveals a peak centered at 226 nm with a long tail out to 280 nm. In contrast, the major peak in the action spectrum measured for **A-ONO** (Figure 5c, blue circles) is shifted to the red at 230 nm and features a broad shoulder at 240 nm that continues to 320 nm (scaled UVPD action spectrum clearly showing the positioning of the major features of these spectra are presented in supplementary materials, Figure S1). Within the uncertainty of the experiment, the action spectrum measured for the authentic nitrobenzene (**A-NO₂**) (Figure 5b, red squares) is the same as measured for the $[M + \text{NO}_2]^+$ adduct. In addition, the UVPD action spectra measured for **A-ONO** (Figure 4c) feature significantly higher photoproduct yields than spectra of both the $[M + \text{NO}_2]^+$ adduct and **A-NO₂** (note the relative magnifications shown in Figures 4a-b), consistent with the lower RO-NO bond dissociation energy of **A-ONO**. It is important to note that the UVPD action spectra being compared here were measured consecutively under identical conditions, in order that temporal fluctuations in the laser power or beam profile were minimized.

Taken together, both CID spectra and UVPD action spectra demonstrate that the $[M + \text{NO}_2]^+$ adduct ion generated by reaction of the charge-tagged phenyl radical (**A**) with NO_2 is 4-nitro-*N,N,N*-trimethylbenzaminium cation (**A-NO₂**) and, furthermore, there is no contribution in this ion population from the nitrosoxy isomer *N,N,N*-trimethyl-4-nitrosoxybenzaminium cation (**A-ONO**).

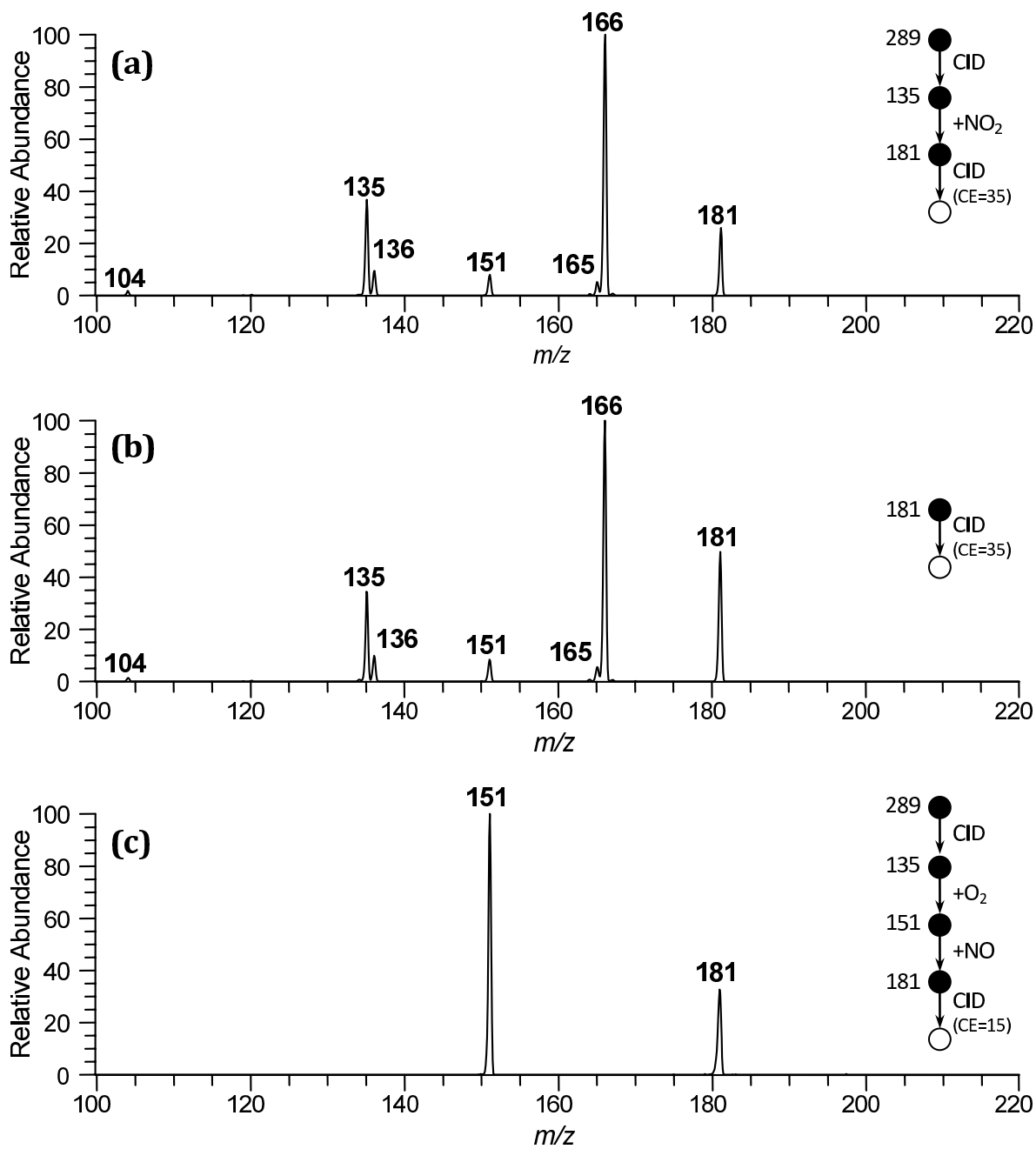


Figure 3 – Comparison of the spectra resulting from CID of the m/z 181 ion generated from (a) the $[\text{M} + \text{NO}_2]^+$ adduct formed after reaction of 4-trimethylammoniumphenyl radical cation (**A**) with NO_2 , (b) genuine 4-nitro- N,N,N -trimethylbenzaminium cation (**A-NO₂**), and (c) N,N,N -trimethyl-4-nitrosoxybenzaminium cation (**A-ONO**).

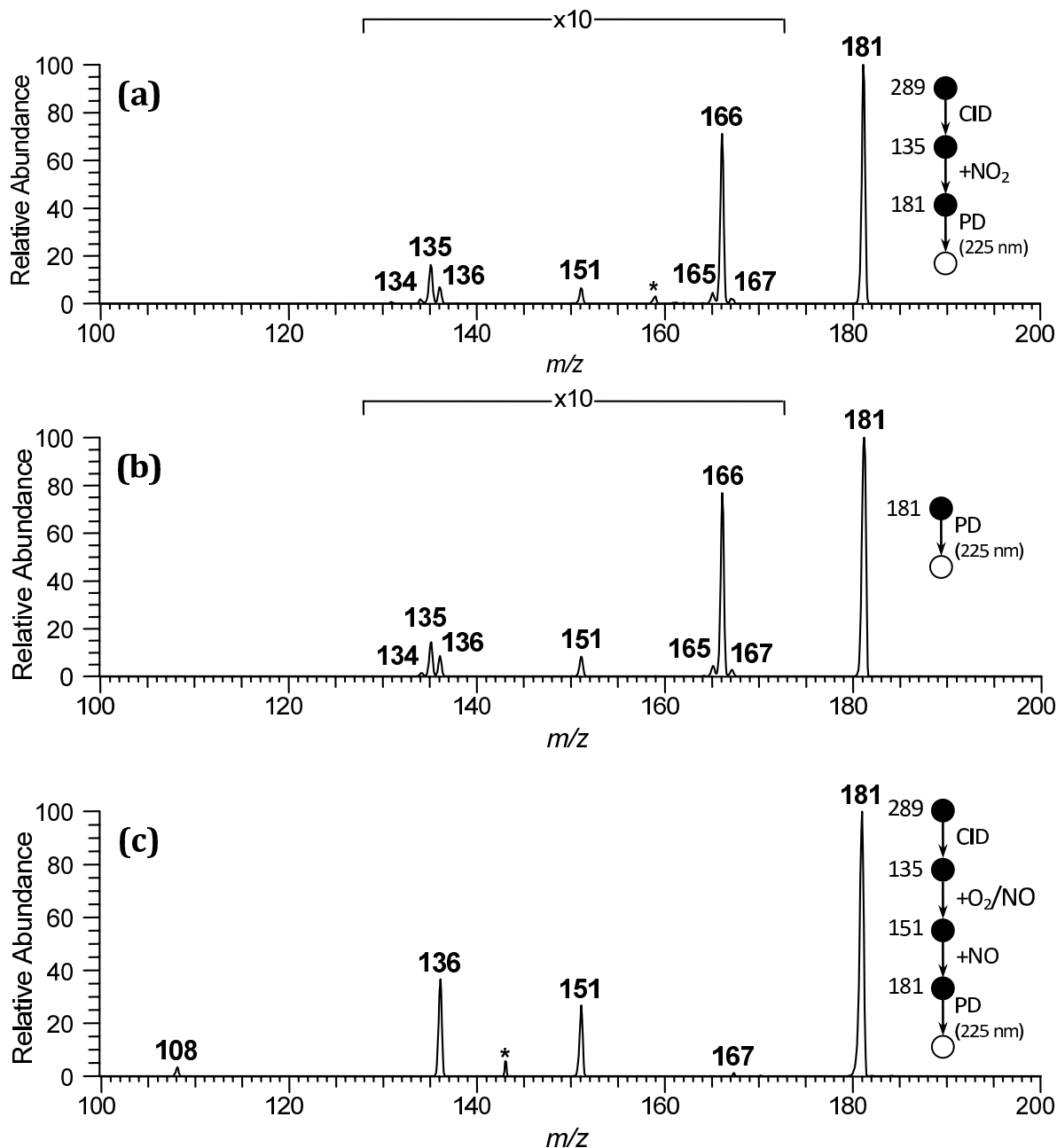


Figure 4 – Comparative UVPD (225 nm) mass spectra of (a) the $[M+NO_2]^+$ adduct generated during reaction of the 4-(*N,N,N*-trimethylammonium)phenyl radical cation with NO_2 , (b) authentic 4-nitro-*N,N,N*-trimethylbenzaminium cation (**A- NO_2**), and (c) 4-nitrosoxy-*N,N,N*-trimethylbenzaminium cation (**A- ONO**). * Ions arising due to laser ablation of the ion-trap back plate or ionization of contaminants.

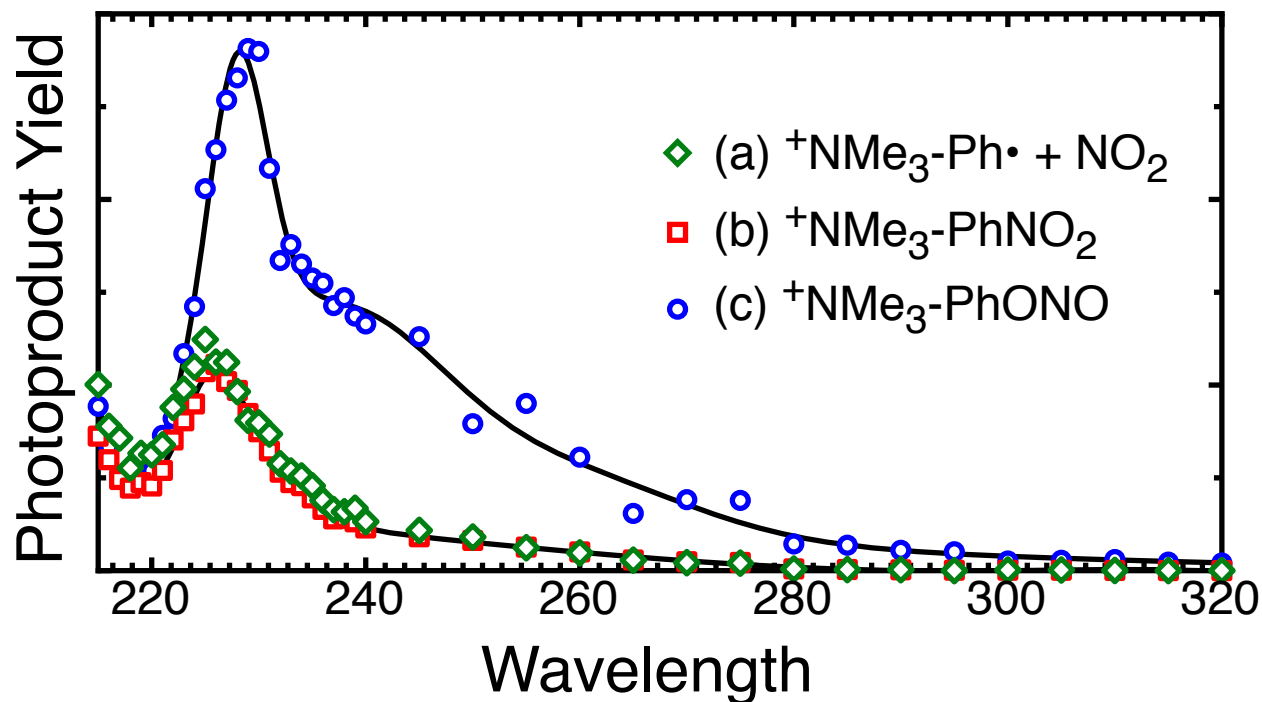
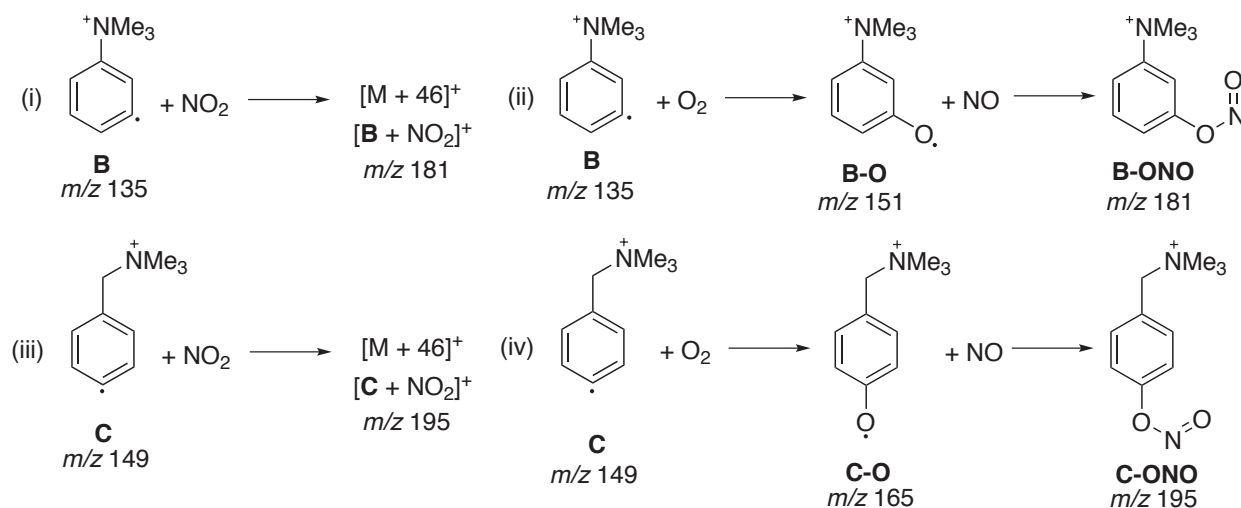


Figure 5 - UVPD action spectrum of (a) the m/z 181 ion generated during reaction of the 4-(*N,N,N*-trimethylammonium)phenyl radical cation with NO_2 (green diamonds), (b) 4-nitro-*N,N,N*-trimethylbenzaminium cation (**A-NO₂**, red squares), and (c) *N,N,N*-trimethyl-4-nitrosoxybenzaminium cation (**A-ONO**, blue circles).

Reaction of two alternative charge-tagged phenyl radical cations with NO₂

In the previous section, we demonstrated that the stabilized $[\text{M} + \text{NO}_2]^+$ adduct formed by the reaction of 4-(*N,N,N*-trimethylammonium)phenyl radical cation (**A**) with NO_2 was exclusively the charge-tagged nitrobenzene (**A-NO₂**). We wished to explore the effect of the charge-tag on this reaction and to investigate whether it is possible to generate a stabilized nitrosoxybenzene (RONO) by modification of the substitution of the phenyl radical. For this purpose, analogous experiments were undertaken with two additional charge-tagged phenyl radical cations generated by 266 nm PD of their respective iodobenzene precursors; (i) 3-(*N,N,N*-trimethylammonium)phenyl radical cation (**B**), where coupling between the charge-tag and radical moiety has been altered by repositioning the $^+\text{NMe}_3$ charge-tag from the *para* to the *meta* position (Scheme 3i-ii); and (ii) 1-(4-

(*N,N,N*-trimethylammonium)methyl)phenyl radical cation (**C**), where the charged moiety is separated from the phenyl ring by a methylene linker (Scheme 3iii-iv). The phenyl radicals **B** and **C** were allowed to react with NO_2 resulting in formation of $[\mathbf{B} + \text{NO}_2]^+$ and $[\mathbf{C} + \text{NO}_2]^+$ ions at m/z 181 and m/z 195, respectively (Scheme 3). The authentic nitrosoxybenzenes **B-ONO** and **C-ONO** were generated by the same method as **A-ONO** (*vide supra*), as depicted in Scheme 3(ii) and (iv), respectively.



Scheme 3 – Outline of the general experiment resulting in isobaric m/z 181 ions arising due to (i) the reaction of 3-(*N,N,N*-trimethylammonium)phenyl radical cation and NO_2 , and authentic (ii) *N,N,N*-trimethyl-3-nitrosoxybenzaminium cation (**B-ONO**), and the isobaric m/z 195 ions arising due to (iii) reaction of 4-((*N,N,N*-trimethylammonium)methyl)phenyl radical cation (**C**) with NO_2 , and authentic (ii) 1-(4-nitrosoxyphenyl)-*N,N,N*-trimethylmethaminium cation (**C-ONO**).

Subjecting the $[\mathbf{B} + \text{NO}_2]^+$ adduct to CID (shown in Figure 6a) resulted in a dominant $[\mathbf{M} - \text{CH}_3]^+$ ion at m/z 166, in addition to minor $[\mathbf{M} - \text{NO}]^+$ and $[\mathbf{M} - \text{NO}_2]^+$ fragment ions at m/z 151 and 135, assigned as the charge-tagged phenoxyl radical and phenyl radical, respectively. This spectrum reveals similar product ions to those present after CID of the corresponding *para*-isomer **A-NO₂** (*c.f.* Figure 3a,c), however, the $[\mathbf{M} - \text{NO} - \text{CH}_3]^+$ ion featured at m/z 136 during CID of **A-NO₂** is absent. This is consistent with the location of the nitro moiety, now at the *meta*-position of the phenyl ring, where the unpaired electron on the nascent phenoxyl radical will no longer be resonantly coupled

to the methyl groups of the $^+\text{NMe}_3$ charge-tag. Subjecting the authentic nitrosoxybenzene (**B-ONO**) to CID results only in an $[\text{M} - \text{NO}]^+$ product ion at m/z 151 ion (shown in Figure 6b). When the collision energy employed for CID of the $[\text{B} + \text{NO}_2]^+$ adduct was reduced to $\text{CE} = 15$ (arbitrary units) in order to compare directly to the CID spectrum of **B-ONO**, there were no products, demonstrating there was no contribution from the nitrosoxy isomer (**B-ONO**) in the $[\text{M} + \text{NO}_2]^+$ ion population. These data suggest reaction of 3-(*N,N,N*-trimethylammonium)phenyl radical cation (**B**) with NO_2 results exclusively in the nitro isomer (**B-NO₂**).

Subjecting the isolated $[\text{C} + \text{NO}_2]^+$ adduct to CID resulted in the mass spectrum depicted in Figure 6(c). An array of product ions is generated, including $[\text{M} - \text{NO}_2]^+$, $[\text{M} - \text{NMe}_3]^+$, $[\text{M} - \text{NO}_2 - \text{CH}_3]^+$, $[\text{M} - \text{NO} - \text{NMe}_3]^+$, $[\text{NMe}_3]^+$ and $[\text{CH}_2=\text{NMe}_2]^+$ ions at m/z 149, 136, 134, 106, 59 and 58, respectively. Interestingly, there is no $[\text{M} - \text{NO}]^+$ ion at m/z 165, instead the majority of the product ions arise due to loss of NO_2 and/or the $^+\text{NMe}_3$ charge-tag. This does not rule out the isomerization channel resulting in ejection of NO , but may instead suggest radical-driven ejection of $^+\text{NMe}_3$ from the nascent phenoxy radical following ejection of NO (analogous to ejection of the CH_3 from $[\text{A-NO}_2 - \text{NO}]^+$). In this case, the positive charge no longer resides with the larger phenoxy-containing fragment. In contrast, CID of the nitrosoxy isomer (**C-ONO**), presented in Figure 6(d), again results only in generation of an $[\text{M} - \text{NO}]^+$ ion at m/z 165.

Overall, there was no evidence for formation of a stabilized nitrosoxybenzene isomer following reaction of either **B** or **C** with NO_2 . The absence of this isomer in the $[\text{M} + \text{NO}_2]^+$ adduct population, and the low CID energy required for ejection of NO from the authentic nitrosoxybenzenes (RONO), may suggest that should the nitrosoxybenzene form, either by direct addition, or isomerization of the nitrobenzene, rapid ejection of NO may follow driven by the large exothermicity of the radical addition reaction.

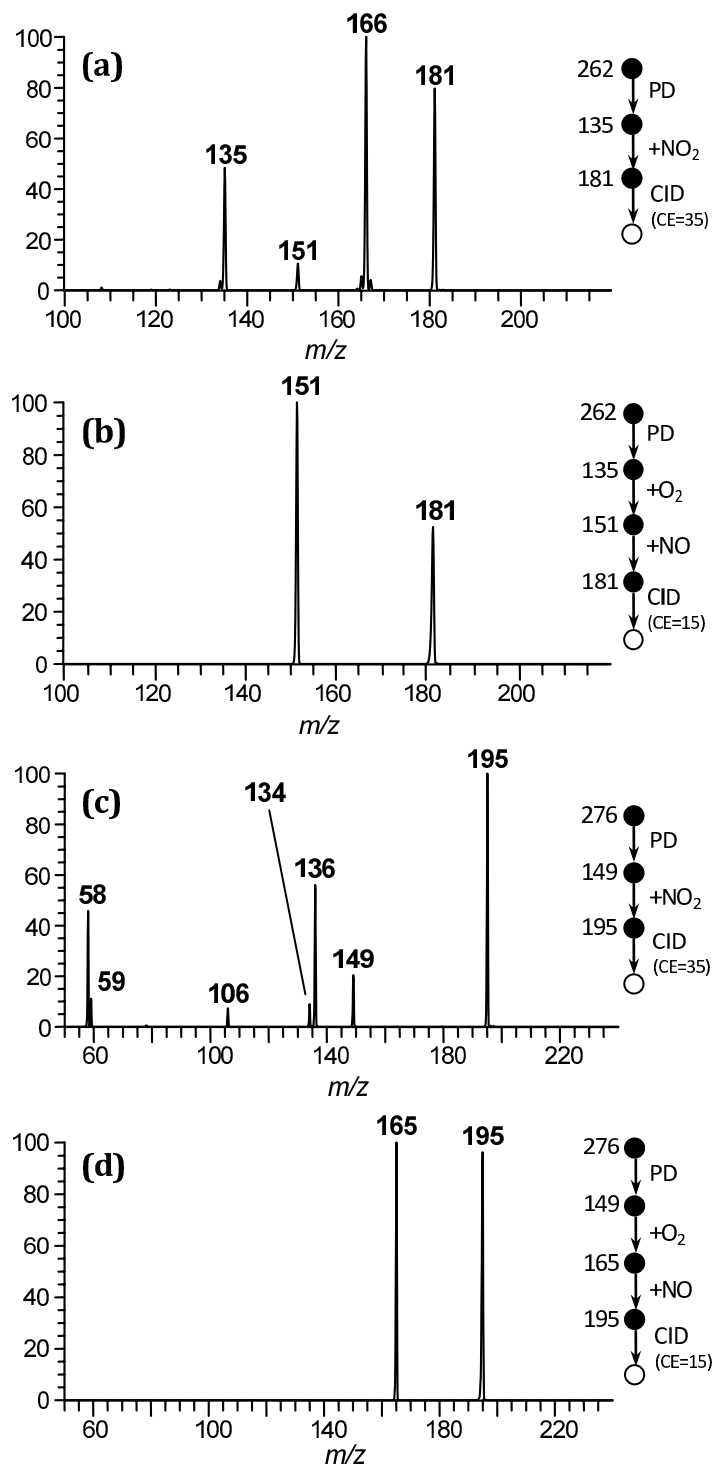


Figure 6 – Mass spectra obtained following CID of the m/z 181 ion generated from (a) reaction of 3-(*N,N,N*-trimethylammonium)phenyl radical cation (**B**) with NO₂, and (b) 3-nitrosoxy-*N,N,N*-trimethylbenzaminium cation (**B-ONO**), and the m/z 195 ion generated from (c) reaction of 4-(*N,N,N*-trimethylammonium)methylphenyl radical cation (**C**) with NO₂, and (d) 1-(4-nitrosoxyphenyl)-*N,N,N*-trimethylmethaminium cation (**C-ONO**).

Calculation of reaction coordinates

We have undertaken electronic structure calculations in an effort to explain the absence of a stabilized nitrosoxybenzene in the $[M + \text{NO}_2]^+$ ion population of all three systems studied and to further elucidate the fragmentation pathways observed during CID of these charge-tagged nitro- (RNO_2) and nitrosoxybenzenes (RONO) . The reaction coordinates of the (i) 4- $(N,N,N$ -trimethylammonium)phenyl radical cation $(\mathbf{A}) + \text{NO}_2$; and (ii) 4- $(N,N,N$ -trimethylammonium)methyl)phenyl radical cation $(\mathbf{C}) + \text{NO}_2$ reactions are depicted in Figures 7 and 8, respectively. The initial addition of NO_2 to \mathbf{A} (Figure 7) proceeds without barrier to generate $\mathbf{A-NO}_2$ with a reaction exothermicity of 60 kcal/mol. Isomerization to the nitrosoxybenzene $(\mathbf{A-ONO})$ requires surmounting a significant barrier of 57 kcal/mol with a reaction exothermicity of 66 kcal/mol relative to the entrance channel. The free energy barrier $(\Delta G_{298}^\ddagger)$ for this isomerization is similar in height to the internal energy barrier (ΔH_0^\ddagger) at 56 kcal/mol, but resides around 9 kcal/mol above the entrance channel. Should the nitrosoxybenzene form, ejection of NO requires only 24 kcal/mol of energy suggesting that trapping significant populations of stabilized nitrosoxybenzenes (RONO) in this potential well following isomerization is unlikely, consistent with these experiments.

These electronic structure calculations also provide a clear rationale for the CID spectra of $\mathbf{A-NO}_2$ and $\mathbf{A-ONO}$ (Figures 4a and 4b, respectively). The major fragments observed during CID of $\mathbf{A-NO}_2$ are loss of CH_3 and NO_2 in accord with the potential energy surface where loss of both CH_3 and NO_2 from $\mathbf{A-NO}_2$ are predicted to require less energy than isomerization to $\mathbf{A-ONO}$, with reaction endothermicities of 51 kcal/mol and 60 kcal/mol, respectively. The significant isomerization barrier to formation of the nitrosoxybenzene $(\mathbf{A-ONO})$ explains the low abundance of the $[\text{M} - \text{NO}]^+$ and $[\text{M} - \text{NO} - \text{CH}_3]^+$ product ions during CID of $\mathbf{A-NO}_2$ and their complete absence at low collision

energies. Ejection of NO after preliminary loss of CH₃ is not predicted to be energetically feasible, as the R-NO₂ to R-ONO barrier of the demethylated nitrobenzene resides 35 kcal/mol above the entrance channel (calculations reported in Supporting Information). When **A-ONO** is formed after isomerization, however, the significant internal energy (66 kcal/mol) should drive prompt ejection of NO (24 kcal/mol) and subsequent loss of CH₃ (which requires only an additional 26 kcal/mol). As discussed above, loss of NO from **A-ONO** is the lowest energy process from this isomer, which is consistent with the observation of exclusive NO loss when **A-ONO** is subjected to CID. No additional product ions are observed in this case, as ejection of NO will proceed before the parent ion gains sufficient energy to explore alternative fragmentation channels. The significant differences in the collision energy required for fragmentation of **A-NO₂** (CE=35 arbitrary units) and **A-ONO** (CE=15 arbitrary units) are clearly consistent with the relative reaction energies of these fragmentation processes.

Despite separating the charge-tag from the phenyl ring by a methylene linker, these calculations suggest addition of NO₂ to **C** to form the nitrobenzene (**C-NO₂**), its isomerization to the nitrosoxybenzene (**C-ONO**) and ejection of NO, are similar in energy to the **A** + NO₂ reaction surfaces (shown in Figure 8). Noticeably, these calculations predict an increase in reaction endothermicity for loss of CH₃ (67 kcal/mol), consistent with its absence during CID of **C-NO₂**. Instead, loss of NMe₃ to form the 4-nitrotoluene cation is lower in energy, at 56 kcal/mol, as is ejection of NO₂ to reform the phenyl radical (**C**). The energy required for ejection of NO from **C-ONO** is 22 kcal/mol lower than for other fragmentation pathways from this isomer. This is consistent with the CID spectrum of **C-ONO** where NO loss was the solitary fragmentation channel. Isomerization of **C-NO₂** to **C-ONO** proceeds with a similar barrier to that of **A-NO₂** at 57 kcal/mol with an overall reaction exothermicity of 66 kcal/mol. Should ejection of NO follow, the considerable excess internal energy of the nascent phenoxy radical (35 kcal/mol) will drive subsequent ejection of ⁺NMe₃, which requires only 24 kcal/mol. This fragmentation channel is

favored over both CH₃ and NMe₃ loss, which in this case require significantly more energy at 59 kcal/mol and 55 kcal/mol, respectively.

Overall, these calculations suggest that isomerization of the nascent nitrobenzene to the nitrosoxybenzene during reaction of the charge-tagged phenyl radical with NO₂ is unlikely, as the free energy barrier for this reaction pathway resides above the entrance channel. This result supports experiments of the charge-tagged phenyl + NO₂ reaction where X-ONO (X = A, B, C) was not detected. Furthermore, in the case of A + NO₂, ejection of CH₃ from A-NO₂ proceeds at a lower energy than isomerization to the nitrosoxybenzene (A-ONO), as such, one would expect these product channels to be competitive with isomerization, which is clearly not the case, as indicated by the absence of an [M - CH₃]⁺ ion in Figure 1. As was previously noted by Glenewinkel-Meyer and Crim [36] for the analogous neutral reaction, should nitrobenzene isomerize to nitrosoxybenzene, the exothermicity of this reaction would easily drive ejection of NO, thus, it would be unlikely to observe a stabilized nitrosoxybenzene product from this reaction.

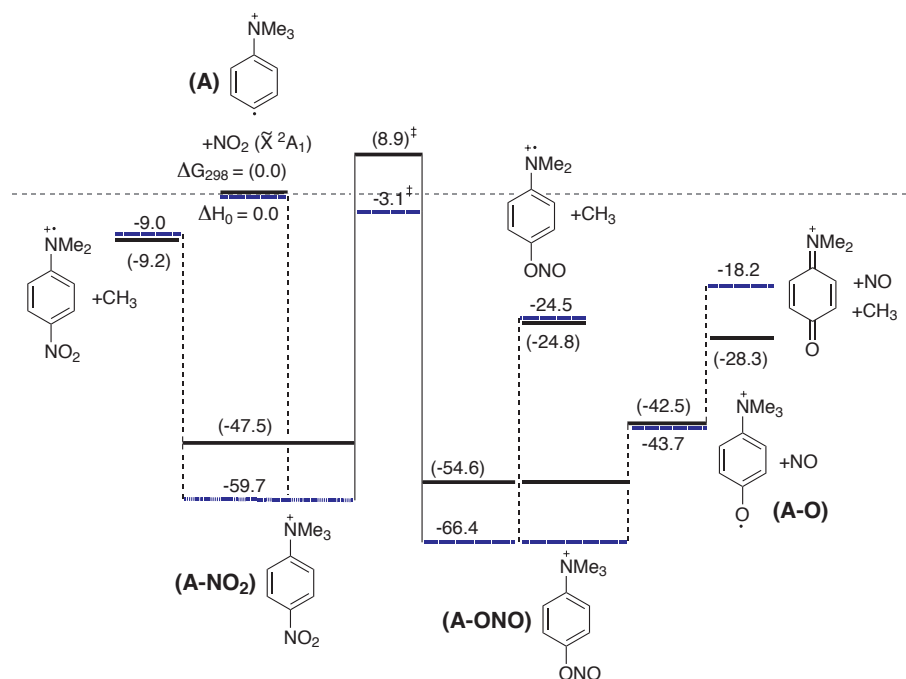


Figure 7 – Potential energy surface of the 4-(*N,N,N*-trimethylammonium)phenyl radical cation (**A**) + NO₂ calculated at the B3LYP/aug-cc-pVDZ level. Solid lines are the Gibbs free energy values (ΔG_{298}) while the hashed blue lines are the energies with zero-point energy correction (ΔH_0). Energies are given in kcal/mol.

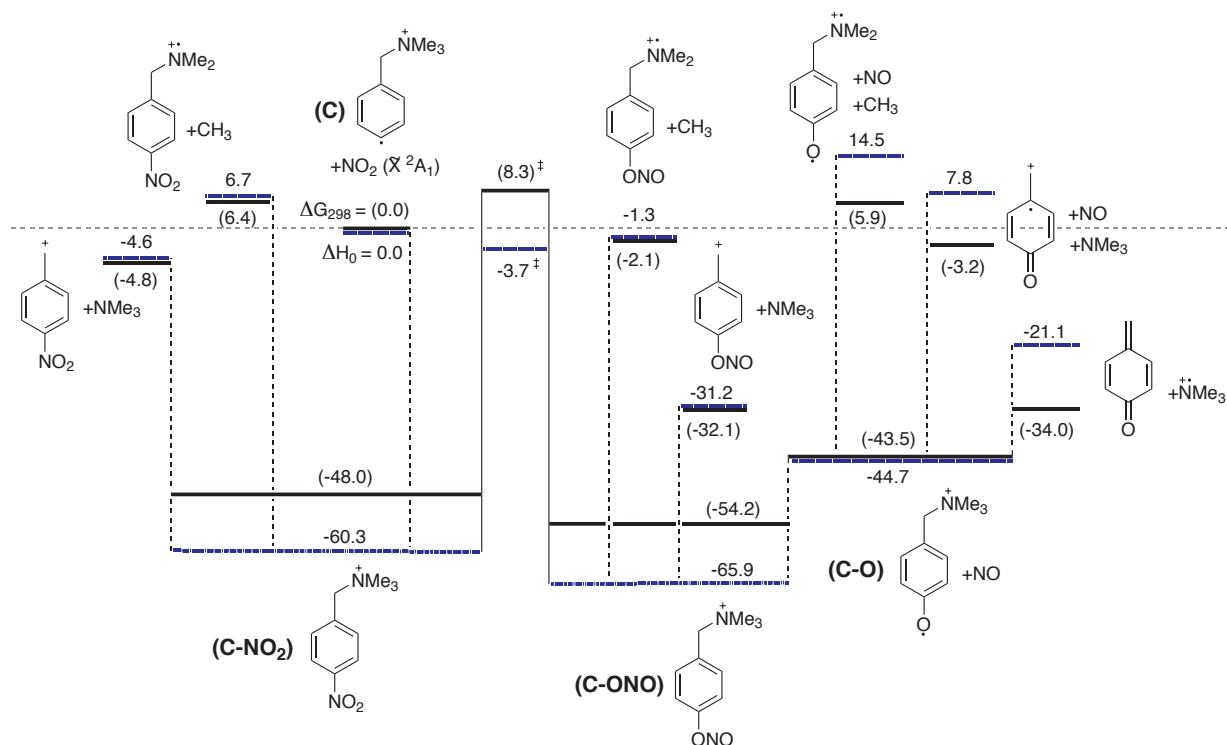


Figure 8 – Potential energy surface of the 4-(*N,N,N*-trimethylammonium)methyl)phenyl radical cation (**C**) + NO₂ calculated at the B3LYP/aug-cc-pVDZ level. Solid lines are the Gibbs free energy values (ΔG_{298}) while the hashed blue lines are the energies with zero-point energy correction (ΔH_0). Energies are given in kcal/mol.

Conclusion

We have successfully investigated the reaction of phenyl radicals with NO₂ using distonic radical models. CID and UVPD action spectroscopy of (i) the [M + 46]⁺ product ion generated during this reaction, and authentic charge-tagged (ii) nitrobenzene and (iii) nitrosoxybenzene isomers, demonstrated unequivocally that the [M + NO₂]⁺ reaction product was nitrobenzene, not the nitrosoxybenzene isomer. These results compare well with the computational study of Xu and Lin [4], where under low-pressure conditions, formation of nitrosoxybenzene is primarily expected to

dissociate to the phenoxy radical ($R + NO_2 \rightarrow [RONO]^* \rightarrow RO + NO$), consistent with its absence during our experiments.

CID of the authentic charge-tagged nitrobenzene and nitrosoxybenzene resulted in significantly different mass spectra. The observation of ions arising due to NO ejection and concomitant fragmentation processes, *e.g.*, CH_3 loss from the charge-tag, was diagnostic for isomerization of the nitrobenzene to the nitrosoxybenzene. Electronic structure calculations suggest the significant internal energy of the nascent nitrosoxybenzene formed after isomerization of the nitrobenzene is sufficient to drive ejection of NO and additional fragmentation pathways. This was in direct contrast to CID of the authentic nitrosoxybenzene, where no excess internal energy is anticipated as CID results in slow heating of the ions and, thus, predominantly dissociation *via* the lowest energy fragmentation channels.

The question arises as to whether these experimental data may help identify the ionized peptidyl radical + NO_2 adduct generated by Barlow *et al.* [9] and to elucidate the fragmentation pathways observed therein. A recent computational study of the ethyl + NO_2 reaction suggested that loss of HONO, the major product ion detected during CID of the peptidyl radical + NO_2 adduct, may proceed *via* the intermediacy of nitroethane ($RNO_2 \rightarrow R' + HONO$) [5]. The barrier for this reaction channel was calculated at 42.8 kcal/mol, in contrast to the significant barrier to nitro-nitrosoxyethane isomerization of 60.7 kcal/mol. In direct comparison to our experiments (*vide supra*), we would hypothesize that the peptidyl radical + NO_2 adduct isolated is a nitroalkane, which would favor ejection of HONO. Competitive isomerization to the nitrosoxyalkane would result in ejection of NO and the excess internal energy of the nascent alkoxy radical could then presumably drive the additional fragmentation channels observed.

Overall, we expect stabilization of a nitrosoxyalkane or nitrosoxyarene (RONO) to be dependent on the energy required for NO ejection. Observation of a stabilized RONO under low-pressure

conditions would only be expected when the energy required for ejection of NO or other low energy fragmentation pathways from RONO rises close to, or above, the R + NO₂ entrance channel.

Acknowledgements

BBK was supported through an Australian Postgraduate Award. The authors acknowledge the financial support of the Australian Research Council (DP0986738, DP0452849), ARC Centre of Excellence for Free Radical Chemistry and Biotechnology (CE0561607) and the University of Wollongong. The authors thank Christopher Hansen (UOW) for assistance with the LTQ + OPO instrumentation, in addition to Intersect (NSW, Australia) and the NCI National Facility (Canberra, Australia) for a generous allocation of resources under the Merit Allocation Schemes.

References

1. Geppert, W. D.; Eskola, A. J.; Timonen, R. S.; Halonen, L. Kinetics of the Reactions of Vinyl (C₂H₃) and Propargyl (C₃H₃) Radicals with NO₂ in the Temperature Range 220-340 K. *J. Phys. Chem. A* **108**, 4232-4238 (2004)
2. Rissanen, M. P.; Arppe, S. L.; Eskola, A. J.; Tammi, M. M.; Timonen, R. S. Kinetics of the R + NO₂ Reactions (R = *i*-C₃H₇, *n*-C₃H₇, *s*-C₄H₉, and *t*-C₄H₉) in the Temperature Range 201-489 K. *J. Phys. Chem. A* **114**, 4811-4817 (2010)
3. Rissanen, M. P.; Popli, K.; Timonen, R. S. Kinetics of resonance stabilized CH₃CCCH₂ radical reactions with NO and NO₂. *Chem. Phys. Lett.* **543**, 28-33 (2012)
4. Xu, S.; Lin, M. C. Computational Study on the Kinetics and Mechanism for the Unimolecular Decomposition of C₆H₅NO₂ and the Related C₆H₅ + NO₂ and C₆H₅O + NO Reactions. *J. Phys. Chem. B* **109**, 8367-8373 (2005)
5. Wang, Q.; Ng, D.; Mannan, M. S. Study on the Reaction Mechanism and Kinetics of the Thermal Decomposition of Nitroethane. *Ind. Eng. Chem. Res.* **48**, 8745-8751 (2009)

6. Weaver, A.; Metz, R. B.; Bradforth, S. E.; Neumark, D. M. Observation of the \tilde{A} (2B_2) and \tilde{C} (2A_2) states of NO_2 by negative ion photoelectron spectroscopy of NO_2^- . *J. Chem. Phys.* **90**(3), 2070-2071 (1989)
7. Ellison, G. B.; Herbert, J. M.; McCoy, A. B.; Stanton, J. F.; Szalay, P. G. Unimolecular Rearrangement of *trans*-FONO to FNO_2 . A Possible Model System for Atmospheric Nitrate Formation. *J. Phys. Chem. A* **108**, 7639-7642 (2004)
8. Lam, M. A.; Pattison, D. I.; Bottle, S. E.; Keddie, D. J.; Davies, M. J. Nitric Oxide and Nitroxides Can Act as Efficient Scavengers of Protein-Derived Free Radicals. *Chem. Res. Toxicol.* **21**, 2111-2119 (2008)
9. Barlow, C. K.; Wright, A.; Easton, C. J.; O'Hair, R. A. J. Gas-phase ion-molecule reactions using regioselectively generated radical cations to model oxidative damage and probe radical sites in peptides. *Org. Biomol. Chem.* **9**, 3733-3745 (2011)
10. Yinon, J. Mass spectral fragmentation pathways in aminonitrobenzenes. A mass spectrometry/mass spectrometry collision-induced dissociation study. *Org. Mass Spectrom* **25**(11), 599-604 (1990)
11. Yinon, J.; McClellan, J. E.; Yost, R. A. Electrospray Ionization Tandem Mass Spectrometry Collision-induced Dissociation Study of Explosives in an Ion Trap Mass Spectrometer. *Rapid Commun. Mass Spectrom.* **11**, 1961-1970 (1997)
12. Nguyen, V. S.; Vinckier, C.; Hue, T. T.; Nguyen, M. T. Decomposition Mechanism of the Anions Generated by Atmospheric Pressure Chemical Ionization of Nitroanilines. *J. Phys. Chem. A* **109**(48), 10954-10960 (2005)
13. Gierczyk, B.; Grajewski, J.; Zalas, M. Differentiation of fluoronitroaniline isomers by negative-ion electrospray mass spectrometry. *Rapid Commun. Mass Spectrom.* **20**, 361-364 (2006)
14. Fayet, G.; Joubert, L.; Rotureau, P.; Adamo, C., Theoretical Study of the Decomposition Reactions in Substituted Nitrobenzenes. *J. Phys. Chem. A* **2008**, *112*, 4054-4059.
15. Mattson, B.; Anderson, M.; Mattson, S. *Microscale Gas Chemistry Book*. 3rd ed.; Educational Innovations: p 482 (2003)
16. Kirk, B. B.; Harman, D. G.; Kenttämaa, H. I.; Trevitt, A. J.; Blanksby, S. J. Isolation and characterization of charge-tagged phenylperoxyl radicals in the gas phase: direct evidence for products and pathways in low temperature benzene oxidation. *Phys. Chem. Chem. Phys.* DOI:10.1039/C2CP43507A (*Accepted*)
17. Ly, T.; Kirk, B. B.; Hettiarachchi, P. I.; Poad, B. L. J.; Trevitt, A. J.; da Silva, G.; Blanksby, S. J. Reactions of simple and peptidic alpha-carboxylate radical anions with dioxygen in the gas phase. *Phys. Chem. Chem. Phys.* **13**, 16314-16323 (2011)

18. Kim, T.-Y.; Thompson, M. S.; Reilly, J. P. Peptide photodissociation at 157nm in a linear ion trap mass spectrometer. *Rapid Commun. Mass Spectrom.* **19**, 1657-1665 (2005)
19. Harman, D. G.; Blanksby, S. J. Investigation of the gas phase reactivity of the 1-adamantyl radical using a distonic radical anion approach. *Org. Biomol. Chem.* **5**, 3495-3503 (2007)
20. Hansen, C. S.; Kirk, B. B.; Blanksby, S. J.; O'Hair, R. A. J.; Trevitt, A. J., Photodissociation Action Spectroscopy with a Linear Ion-Trap Mass Spectrometer. *Submitted*.
21. Kirk, B. B.; Trevitt, A. J.; Blanksby, S. J.; Tao, Y.; Moore, B. N.; Julian, R. R. Ultraviolet Action Spectroscopy of Iodine Labeled Peptides and Proteins in the Gas Phase. *J. Phys. Chem. A*, DOI: 10.1021/jp305470j (*Accepted*).
22. Gronert, S. Estimation of Effective Ion Temperatures in a Quadrupole Ion Trap. *J. Am. Soc. Mass Spectrom.* **9**, 845-848 (1998)
23. Becke, A. D. A new mixing of Hartree-Fock and local density-functional theories. *J. Chem. Phys.* **98**, 1372 (1993)
24. Lee, C.; Yang, W. T.; Parr, R. G. Development of the {Colle-Salvetti} correlation-energy formula into a functional of the electron density. *Phys. Rev. B: Condens. Matter* **37**(2), 785-789 (1988)
25. Dunning, T. H., Jr. Gaussian basis sets for use in correlated molecular calculations. I. The atoms boron through neon and hydrogen. *J. Chem. Phys.* **90**, 1007-1023 (1989)
26. Frisch, M. J.; Trucks, G. W.; Schlegel, H. B.; Scuseria, G. E.; Robb, M. A.; Cheeseman, J. R.; Scalmani, G.; Barone, V.; Mennucci, B.; Petersson, G. A.; Nakatsuji, H.; Honda, Y.; Kitao, O.; Nakai, H.; Vreven, T.; Montgomery, J., J. A.; Peralta, J. E.; Ogliaro, F.; Bearpark, M.; Heyd, J. J.; Brothers, E.; Kudin, K. N.; Staroverov, V. N.; Keith, T.; Kobayashi, R.; Normand, J.; Raghavachari, K.; Rendell, A.; Burant, J. C.; Iyengar, S. S.; Tomasi, J.; Cossi, M.; Rega, N.; Millam, J. M.; Klene, M.; Knox, J. E.; Cross, J. B.; Bakken, V.; Adamo, C.; Jaramillo, J.; Gomperts, R.; Stratmann, R. E.; Yazyev, O.; Austin, A. J.; Cammi, R.; Pomelli, C.; Ochterski, J. W.; Martin, R. L.; Morokuma, K.; Zakrzewski, V. G.; Voth, G. A.; Salvador, P.; Dannenberg, J. J.; Dapprich, S.; Daniels, A. D.; Farkas, O.; Foresman, J. B.; Ortiz, J. V.; Cioslowski, J.; Fox, D. J. *Gaussian 09*, Revision C.01; Gaussian, Inc.: Wallingford CT (2010)
27. Hratchian, H. P.; Schlegel, H. B. Accurate reaction paths using Hessian based predictor-corrector integrator. *J. Chem. Phys.* **120**, 9918-9924 (2004)
28. Hratchian, H. P.; Schlegel, H. B. In *Theory and Applications of Computational Chemistry: The First 40 Years*, E., D. C.; Frenking, G.; Kim, K. S.; Scuseria, G. E., Eds. Elsevier: Amsterdam (2005)
29. Hratchian, H. P.; Schlegel, H. B. Using Hessian updating to increase the efficiency of a Hessian based predictor-corrector reaction path following method. *J. Chem. Theory Comput.* **1**, 61-69 (2005)
30. Kirk, B. B. *Investigating the reactions of gas-phase radicals using distonic ions*, PhD Thesis, University of Wollongong (2011)

31. Arey, J.; Aschmann, S. M.; Kwok, E. S. C.; Atkinson, R. Alkyl Nitrate, Hydroxylalkyl Nitrate, and Hydroxycarbonyl Formation from the NO_x-Air Photooxidations of C₅-C₈ *n*-Alkanes. *J. Phys. Chem. A* **105**, 1020-1027 (2001)
32. Yu, T.; Mebel, A. M.; Lin, M. C. Reaction of phenoxy radical with nitric oxide. *J. Phys. Org. Chem.* **8**(1), 47-53 (1995)
33. Berho, F.; Caralp, F.; Rayez, M.-T.; Lesclaux, R.; Ratajczak, E. Kinetics and Thermochemistry of the Reversible Combination Reaction of the Phenoxy Radical with NO. *J. Phys. Chem. A* **102**(1), 1-8 (1998)
34. Platz, J.; Nielsen, O. J.; Wallington, T. J.; Ball, J. C.; Hurley, M. D.; Straccia, A. M.; Schneider, W. F. Atmospheric Chemistry of the Phenoxy Radical, C₆H₅O(•): UV Spectrum and Kinetics of Its Reaction with NO, NO₂, and O₂. *J. Phys. Chem. A* **102**(41), 7964-7974 (1998)
35. McLuckey, S. A.; Goeringer, D. E. Slow Heating Methods in Tandem Mass Spectrometry. *J. Mass Spectrom.* **32**, 461-474 (1997)
36. Glenewinkel-Meyer, T.; Crim, F. F. The isomerization of nitrobenzene to phenylnitrite. *J. Mol. Struct. (THEOCHEM)* **337**, 209-224 (1995)